An X-Band Oscillator Utilizing Overtone Lithium Niobate MEMS Resonator and 65-nm CMOS

Ali Kourani, Yansong Yang, and Songbin Gong
Department of Electrical and Computer Engineering
University of Illinois at Urbana-Champaign, Urbana, IL, USA

***Abstract*— This paper presents an 8.6 GHz oscillator utilizing a third antisymmetric overtone (A_3) in a lithium niobate ($LiNbO_3$) resonator for 5G communications. The oscillator consists of an acoustic resonator in a closed loop with cascaded RF tuned amplifiers (TAs) built on TSMC RF GP 65 nm CMOS. The TAs bandpass response, set by on-chip inductors, satisfies the Barkhausen's oscillation conditions for A_3 while suppressing the fundamental and higher-order resonances. The oscillator achieves a measured phase noise of -56 and -113 dBc/Hz at 1 kHz and 100 kHz offsets from an 8.6 GHz output while consuming 10.2 mW of dc power. The oscillator also attains a figure-of-merit of 201.6 dB at 100 kHz offset, surpassing the state-of-the-art (SoA) EM and RF-MEMS oscillators.**

***Keywords*— lithium niobate; MEMS; overtone; oscillator;**

I. Introduction

Currently, the sub-3 GHz frequency bands are too congested to meet the ever-increasing data rates demanded by many cellular users. The call for higher bandwidths and speeds has pushed the 5G radios towards mm-wave frequencies. In the meantime, 5G wireless transceivers are expected to feature higher sensitivity and selectivity while producing longer battery life, all in small form factors.

To achieve all the above, high-performance chip-scale RF synthesizers beyond 3 GHz are highly sought after. State-of-the-art (SoA) microwave oscillators are based on on-chip LC [1], microstrip [2], active [3], and dielectric resonators (DR) [4]. On-chip *LC* tanks are compact but lossy, hence offering a low-cost but low-performance solution. Their low-quality factor (Q) at microwave frequencies translates to poor phase noise and high-power consumption. Quarter wavelength electromagnetic (EM) resonators have footprints on the order of 9 mm for an 8 GHz resonance, making them too bulky for handsets. DROs offer superior phase noise performance, but they are bulky and consume a large amount of power.

Alternatively, oscillators based on microelectromechanical (MEMS) resonators are attractive for portable devices as they have low phase noise and low power consumption. Moreover, they harness the resonance in the acoustic domain, leading to a much more compact size. Recently, acoustic resonators with resonances above 8 GHz have been demonstrated in different platforms such as aluminum nitride (AlN) thin-film bulk acoustic resonators (FBARs) [5], AlN contour mode resonators (CMRs) [6][7], scandium doped AlN resonators [8][9], ferroelectric resonators [10], FinFET resonators [11], and lithium niobate ($LiNbO_3$) resonators [12]-[15]. From this group, $LiNbO_3$ resonators feature the highest figure-of-merit ($FoM_{RES} = Q \times$ electromechanical coupling coefficient, k_t^2), making them the most suitable candidate for enabling chip-scale oscillators with simultaneously low phase noise and low power consumption [16]-[18].

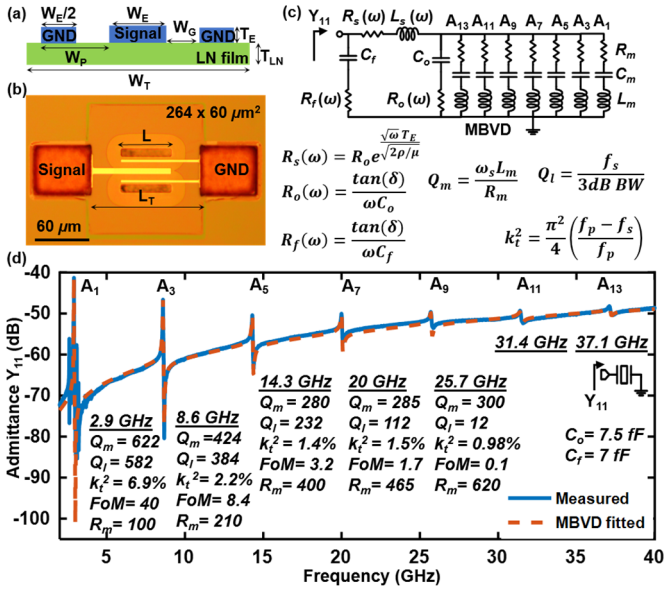

Fig. 1. (a) Mockup cross-sectional view of the $LiNbO_3$ resonator with key parameters are shown. W_T= 32 μm, W_G= 6 μm, W_E= 8 μm, T_E= 180 nm, thickness of the electroplated Cu pad is 3 μm, T_{LN}= 650 nm, L_T= 140 μm, L= 60 μm, and pad area is 60 x 62 μm^2. (b) Optical image of the fabricated resonator. (c) Multi-resonance equivalent MBVD model with parasitics included. (d) Measured and MBVD fitted response for the first 7 odd modes. tan(δ) is the loss tangent of $LiNbO_3$, ρ is the resistivity of the Cu thin-film, and μ is the permeability of Cu. Mechanical (Q_m), loaded (Q_l) quality factors, k_t^2, FoM, and R_m of each tone are shown.

To this end, this paper presents an X-band oscillator utilizing a third antisymmetric overtone (A_3) in a $LiNbO_3$ RF-MEMS resonator and 65 nm CMOS. The oscillator achieves a measured phase noise of -56, -113, and -135 dBc/Hz at 1 kHz, 100 kHz, and 1 MHz offsets from an 8.6 GHz output while consuming 10.2 mW of dc power. The oscillator also attains a figure-of-merit of 201.6 dB at 100 kHz offset, surpassing the SoA X-band EM oscillators [1]-[4] and RF-MEMS oscillators above 5 GHz [15], [19]-[22].

II. Oscillator Design

As shown in Figs. 1(a) and (b), the resonator is comprised of a 3-electrode transducer on top of a mechanically suspended Z-cut $LiNbO_3$ thin-film is. The electrodes are connected to signal and ground to induce lateral electric fields in the piezoelectric film, hence exciting the resonator into odd-order antisymmetric vibrations.

978-1-7281-6430-4/20/$31.00 ©2020 IEEE

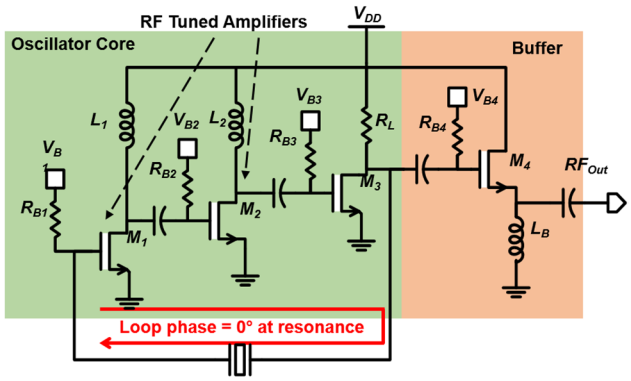

Fig. 2. Schematic of the 8.6 GHz oscillator core and buffer.

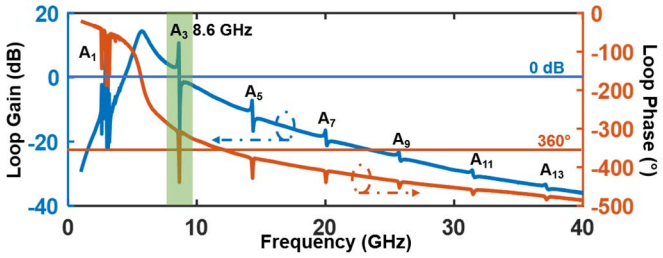

Fig. 3. Post-layout simulated loop gain and phase. Only the A_3 resonance satisfies the Barkhausen's conditions of oscillation. Measured S-parameters of the resonator is used in this simulation.

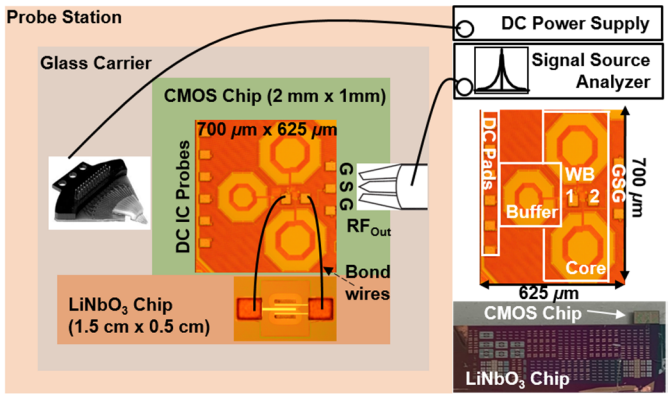

Fig. 4. Measurement setup.

The resonator is fabricated with the dimensions in the inset of Fig. 1, and using a process described in [12].

A multi-resonance modified Butterworth-Van Dyke (MBVD) model shown in Fig. 1(c) is used to interpret the measured admittance shown in Fig. 1(d). The third antisymmetric mode, A_3, is characterized by a mechanical quality factor (Q_m) of 424, a loaded quality factor (Q_l) of 384, a k_t^2 of 2.2%, and a FoM_{RES} of 8.4. The resonator has a total capacitance of 14.5 fF, which includes both the static capacitance from IDT, C_o, and feedthrough capacitance, C_f.

The oscillator consists of the resonator in a closed loop with two inductively-loaded NMOS common source (CS) tuned amplifiers (TAs) and a final resistively-loaded NMOS CS stage. All stages are ac coupled independently to provide bias for the transistors and low noise performance. The oscillator schematic is shown in Fig. 2. The TA bandpass response is determined by the loading inductors (L_1 and L_2). The inductance

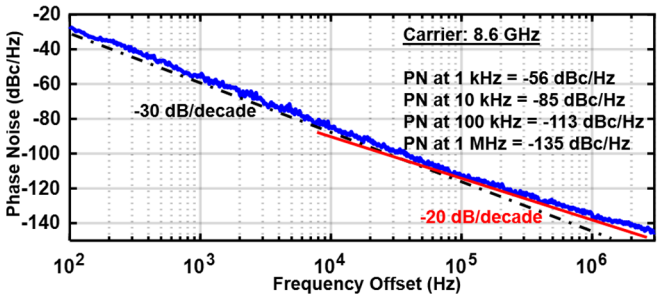

Fig 5. Measured phase noise of the 8.6 GHz carrier.

TABLE I. COMPARISON TO SOA RF-MEMS OSCILLATORS ABOVE 5 GHZ

		This work	[15]	[19]	[20]	[21]
Resonator		**$LiNbO_3$ A_3**	$LiNbO_3$ A_3	FBAR fundamental	FBAR fundamental	FBAR 3rd tone
IC Process		**65 nm CMOS**	Discrete	0.35 μm BiCMOS	Discrete	Discrete
Osc. Freq. (GHz)		**8.6**	12.9	5.46	5	7
Resonator Footprint (mm^2)		**0.016**	0.01	0.034	> 0.1	-
Q_l		**384**	270	300#	300	1350
k_t^2 (%)		**2.2**	1.9	6.67#	4.3	-
FoM_{RES}		**8.4**	5.1	20	12.9	-
dc Power (mW)		**10.2**	20	12.7	-	16.2
PN (dBc/Hz)	1 kHz	**-56**	-70	-64^	-	-
			-73.5	-60	-	-
	100 kHz	**-113**	-111	-117.7	-109.5	-80
			-114.5	-113.8	-104.8	-78.2
	1 MHz	**-135**	-131	-	-	-110
			-134.5	-	-	-108.2
FoM_{Osc} (dB)	100 kHz	**201.6**	200.2	201.4	-	164.8

The values in the shaded cells are referenced to an 8.6 GHz output. # as reported in [22]. ^ value estimated from a plot in [19]. $FoM_{OSC} = -L(\Delta f) + 20\,log\left(\frac{f_o}{f_m}\right) - 10\,log\left(\frac{P_{dc}}{1\,mW}\right)$, where $L(\Delta f)$ is the phase noise measured at an offset f_m from a carrier f_o, and P_{dc} is the dc power consumption.

values are chosen for a gain peak at 5.7 GHz, a frequency between A_1 (2.9 GHz) and A_3 (8.6 GHz). This bandpass response excites A_3 and suppresses A_1 and higher-order resonances, as shown in Fig. 3. L_1 and L_2 minimally affect Q_l since their center frequencies are far from 8.6 GHz. A low-power source-follower stage is used for 50 Ω-based measurements.

III. MEASUREMENTS

The TSMC RF GP 65 nm CMOS chip (2 mm × 1 mm) is integrated with the MEMS chip (1.5 cm × 0.5 cm) on a glass substrate via wire bonding. The CMOS circuitry occupying an area of 700 μm × 625 μm is shown in Fig.4. The oscillator was tested on a probe station where the output was sensed using a 100 μm pitch GSG probe. DC probes with decoupling capacitors was used to deliver the transistor bias voltages. Probing was planned as the measurement method in the design stage to avoid complications from parasitic inductances added to L_1 and L_2. Phase noise measurements were taken using Rohde & Schwarz FSUP26 signal analyzer and reported in Fig. 5. The oscillator achieves a measured phase noise of -56 and -113 dBc/Hz at 1 kHz and 100 kHz offsets from an 8.6 GHz carrier while consuming 10.2 mW of dc power.

TABLE II. COMPARISON TO SOA EM OSCILLATORS

		This work	[4]			[2]	[3]	[1]
Resonator		**$LiNbO_3$**	DRO			µstrip	Active	LC
IC Process		**65 nm CMOS**	GaN	GaAs	SiGe	BJT	Discrete	BiCMOS
Osc. Freq. (GHz)		**8.6**	10.6			10	10	15
Resonator Footprint (mm^2)		**0.016**	-			-	-	-
Q_l		**384**	600			-	1211	-
dc Power (mW)		**10.2**	-			200	500	72
PN (dBc/Hz)	1 kHz	**-56**	-53††	-76††	-90††	-65†	-	-
			-54.8	-77.8	-91.8	-66.3		
	100 kHz	**-113**	-118	-123	-135	-113	-114.4	-102*
			-119.8	-124.8	-136.8	-114.3	-115.7	-106.8
FoM_{Osc} (dB)	100 kHz	**201.6**	-			190	187.4	187

The values in the shaded cells are referenced to an 8.6 GHz output. †† Values are estimated from a plot in [4]. † Values are estimated from a plot in [2]. *Values are estimated from a plot in [1].

IV. CONCLUSIONS

In comparison to the X-band oscillators in Tables I and II, the figure-of-merit (FoM_{OSC}) of our oscillator surpasses those of the SoA EM and RF-MEMS oscillators above 5 GHz. Moreover, the measured oscillation frequency is the highest reported to date for a MEMS oscillator wire-bonded to CMOS. Via tuning the inductive loads (L_1, and L_2), the same oscillator topology can be used to excite higher-order resonances. Moreover, adding an on-chip varactor in parallel to L_1/L_2 can enable the oscillator to hop among different overtones rather than just generating a fixed frequency output. Hence, this approach also allows for a potentially ultra-wideband reconfigurable frequency generation.

ACKNOWLEDGMENT

The authors would like to thank the NSF SpecEES program for funding support.

REFERENCES

[1] F. Padovan, F. Quadrelli, M. Bassi, M. Tiebout, and A. Bevilacqua, "A Quad-Core 15GHz BiCMOS VCO with -124 dBc/Hz Phase Noise at 1MHz Offset, -189dBc/Hz FOM, and Robust to Multimode Concurrent Oscillations," *IEEE Int.Solid-State Circuits Conf.*, 2018, pp. 376-377.

[2] A. Khanna, E. Topacio, E. Gane, and D. Elad, "Low Jitter Silicon Bipolar Based VCOs for Applications in High Speed Optical Communication Systems," *IEEE Int.Microw. Symp*, 2001, pp. 1567- 1570.

[3] Y. Lee, J. Lee, and S. Nam, "High-Q active resonators using amplifiers and their applications to low phase-noise free-running and voltage-controlled oscillators," *IEEE Trans. on Microw. Theory and Techn*., vol. 52, no. 11, pp. 2621- 2626, 2004.

[4] P. Rice, R Sloan, M. Moore, A. Barnes, M. Uren, N. Malbert, and N. Labat, "A 10 GHz dielectric resonator oscillator using GaN technology," *IEEE Int.Microw. Symp*, 2004, pp. 1497- 1500.

[5] M. Hara et al., "Super-High-Frequency Band Filters Configured with Air-Gap-Type Thin," *Jpn. J. Appl. Phys*, vol. 49, no. 7, pp. 07HD13.1-07HD13.4, 2010.

[6] G. Chen and M. Rinaldi, "High-Q X Band Aluminum Nitride Combined Overtone Resonators," *Joint Conference of the IEEE Int. Freq. Control Symp. and European Freq. and Time Forum (EFTF/IFC),* 2019, pp. 1-3.

[7] M. Rinaldi, C. Zuniga, and G. Piazza, "5-10 GHz AlN Contour-Mode Nanoelectromechanical Resonators," *IEEE Int. Conf. on MEMS*, 2009, pp. 916-919.

[8] M. Park, Z. Hao, D. Kim, A. Clark, R. Dargis, and A. Ansari, "A 10 GHz Single-Crystalline Scandium-Doped Aluminum Nitride Lamb-Wave Resonator," *Int. Conf. on Solid-State Sensors, Actuators and Microsys. & Eurosensors XXXIII*, 2019, pp. 450- 453.

[9] M. Park, J. Wang, R. Dargis, A. Clark, and A. Ansari, "Super High-Frequency Scandium Aluminum Nitride Crystalline Film Bulk Acoustic Resonators," *IEEE Int. Ultrasonics Symp. (IUS),* 2019, pp. 1689-1692.

[10] M. Ghatge, G. Walters, T. Nishida, and R. Tabrizian, "High-Q UHF and SHF Bulk Acoustic Wave Resonators with Ten-Nanometer $HF_{0.5}ZR_{0.5}O_2$ Ferroelectric Transducer," *Int. Conf. on Solid-State Sensors, Actuators and Microsys. & Eurosensors XXXIII*, 2019, pp. 450- 453.

[11] D. Weinstein and S. A. Bhave, "Acoustic Resonance in an independent-gate FinFET," Solid-State Sensors, Actuators and Microsystems Workshop, pp. 459- 462, 2010.

[12] Y. Yang, R. Lu, T. Manzaneque, and S. Gong, "Towards Ka band acoustic: lithium niobate asymmetrical mode piezoelectric MEMS resonators," *IEEE Int. Freq. Cont. Symp*., May 2018, pp.1-5.

[13] Y. Yang, R. Lu, and S. Gong, "Scaling Acoustic Filters Towards 5G," *2018 IEEE International Electron Devices Meeting (IEDM)*, San Francisco, CA, 2018, pp. 39.6.1-39.6.4.

[14] V. Plessky et al., "Laterally excited bulk wave resonators (XBARs) based on thin Lithium Niobate platelet for 5GHz and 13 GHz filters," *IEEE MTT-S Int. Microw. Symp. (IMS)*, 2019, pp. 512-515.

[15] A. Kourani, Y. Yang, and S. Gong, "A Ku-Band Oscillator Utilizing Overtone Lithium Niobate RF-MEMS Resonator for 5G," in *IEEE Microw. and Wireless Components Letters*, vol. 30, no. 7, pp. 681-684, July 2020.

[16] A. Kourani and S. Gong, "A tunable low-power oscillator based on high-Q lithium niobate MEMS resonators and 65-nm CMOS," *IEEE Trans. Microw. Theory Techn.,* vol. 66, no. 12, pp. 5708- 5723, 2018.

[17] A. Kourani, R. Lu, A. Gao, and S. Gong, "A 300-500 MHz Tunable Oscillator Exploiting Ten Overtones in Single Lithium Niobate Resonator," *Joint Conf. of the IEEE Int. Freq. Control Symp. and European Freq. and Time Forum (EFTF/IFCS)*, 2019, pp. 1-4.

[18] A. Kourani, R. Lu, and S. Gong, "A Wideband Oscillator Exploiting Multiple Resonances in Lithium Niobate MEMS Resonator," in *IEEE Trans. on Ultrason., Ferroelectr., and Freq. Control*, doi: 10.1109/TUFFC.2020.2989623.

[19] M. Aissi, E. Tournier, M. Dubois, G. Parat, and R. Plana, "A 5.4 GHz 0.35µm BiCMOS FBAR Resonator Oscillator in Above-IC Technology," *IEEE Int.Solid-State Circuits Conf.*, 2006, pp. 1228-1235.

[20] H. Zhang, J. Kim, W. Pang, H. Yu, and E. Kim, "5 GHz Low-phase-noise Oscillator Based on FBAR with Low TCF," *Int. Conf. on Solid-State Sensors, Actuators and Microsystems,* 2005, pp. 1100- 1101.

[21] M. ElBarkouky, G. Vandersteen, P. Wambacq, and Y. Rolain, "A 7 GHz FBAR Overtone–Based Oscillator," *Euro. Microw. Conf.*, 2009, pp. 318-321.

[22] E. Tournier, "5.4GHz, 0.35µm BiCMOS FBAR-Based Single-Ended and Balanced Oscillators in Above-IC Technology," *MEMS-based Circuits and Systems for Wireless Communication, Springer*, pp. 155-186, 2013.